Macromolecules
ARTICLE

Macromolecules **2010**, *43*, 5387–5395 **5387**
DOI: 10.1021/ma100716n

Evolution of Phase Morphology of Mixed Poly(*tert*-butyl acrylate)/Polystyrene Brushes Grafted on Silica Particles with the Change of Chain Length Disparity

Xiaoming Jiang,[†] Ganji Zhong,[‡,§] Jonathan M. Horton,[†] Naixiong Jin,[†] Lei Zhu,[‡] and Bin Zhao*[,†]

[†]*Department of Chemistry, University of Tennessee, Knoxville, Tennessee 37996,* [‡]*Department of Macromolecular Science and Engineering, Case Western Reserve University, Cleveland, Ohio 44106, and* [§]*College of Polymer Science and Engineering, Sichuan University, Chengdu 610065, People's Republic of China*

Received April 2, 2010; Revised Manuscript Received May 10, 2010

ABSTRACT: We report in this article the synthesis of a series of mixed poly(*tert*-butyl acrylate) (P*t*BA)/polystyrene (PS) brushes with P*t*BA number-average molecular weight (M_n) being fixed at 24.5 kDa and PS M_n ranging from 14.8 to 30.4 kDa on 160 nm silica particles and the study of their microphase separation behaviors using differential scanning calorimetry (DSC) and transmission electron microscopy (TEM). The samples were synthesized by a two-step "grafting from" process from asymmetric difunctional initiator (Y-initiator)-functionalized silica particles using two different "living"/controlled radical polymerization techniques. P*t*BA brushes were grown first from Y-initiator-functionalized particles by surface-initiated atom transfer radical polymerization of *tert*-butyl acrylate at 75 °C in the presence of a free initiator, followed by nitroxide-mediated radical polymerization (NMRP) of styrene at 120 °C. The "living" nature of NMRP allowed the synthesis of mixed P*t*BA/PS brushes with different PS molecular weights (14.8, 18.7, 24.9, and 30.4 kDa) in a one-pot polymerization. DSC studies showed that all thermally annealed mixed brush samples exhibited two glass transitions with the middle points located at ~47 and ~90 °C, suggesting that the two tethered polymers microphase separated in the brush layer. For TEM studies, the samples were dispersed in $CHCl_3$, a good solvent for both P*t*BA and PS, drop-cast onto carbon films, thermally annealed in vacuum at 120 °C for 3 h, and then stained with RuO_4 vapor. All samples showed clear microphase separation, consistent with the DSC results. With increasing PS M_n from 14.8, to 18.7, and 24.9 kDa, the morphology of mixed brushes evolved from isolated, nearly spherical PS microdomains buried inside the P*t*BA matrix, to short PS cylindrical microdomains in the P*t*BA matrix, and to nearly bicontinuous nanostructures. Further increasing the molecular weight of PS to 30.4 kDa resulted in the formation of isolated P*t*BA microdomains which were covered by PS chains.

Introduction

Binary mixed homopolymer brushes are composed of two chemically distinct homopolymers randomly or alternately immobilized by one end via a covalent bond on the surface of a solid substrate.[1−3] These brushes represent a new, intriguing class of environmentally responsive materials. The two grafted polymers, which are not necessarily stimuli-sensitive, can undergo spontaneous chain reorganization in response to environmental variations and exhibit different nanostructures and surface properties.[1−3] This response mechanism is different from those of traditional stimuli-sensitive, e.g., thermosensitive, polymer brushes where individual polymer chains exhibit different chain structures and properties upon application of an external stimulus.[4] Certainly, the use of stimuli-responsive polymers would further enrich the self-assembly behaviors and responsive properties of mixed brushes.[5]

The phase morphologies and responsive properties of mixed homopolymer brushes have been intensively investigated in the past two decades.[1−3,5−14] Theoretically, Marko and Witten studied whether symmetric mixed brushes on a flat substrate microphase separated laterally or vertically under equilibrium melt conditions and predicted that the lateral phase separation preempted the vertical phase separation, yielding a "rippled" nanostructure instead of a "layered" structure.[1a] The periodicity of the rippled pattern was predicted to be 1.97 times the chain root-mean-square end-to-end distance ($\langle R_{rms} \rangle$). They also pointed out that by altering the compositions and molecular weights of mixed brushes, first-order transitions between different ordered states could be achieved. The lateral phase separation of symmetric mixed brushes under melt or near-melt conditions and in nonselective solvents was also revealed by other researchers in theoretical or simulation studies.[1c,d,2,6,7] In selective solvents, surface-tethered micellar structures with the solvophobic polymer packing into a core and the solvophilic chains forming the corona were predicted.[2d] By tuning parameters, including chain lengths, grafting densities, chemical compositions, solvent quality, and temperature, a variety of surface nanostructures could be formed by mixed brushes.[1−3,6−8] Moreover, different structures formed from the same brushes are fully reversible because of the covalent grafting of polymer chains to the substrate.

Experimentally, many methods have been developed to prepare mixed brushes.[5,9−14] Sidorenko et al. reported the synthesis of first mixed brushes by a two-step surface-initiated conventional free radical polymerization process and demonstrated the switching properties of mixed brushes by treating them with selective solvents.[9] Besides the two-step conventional free radical polymerization,[10] "grafting to" and other "grafting from" methods

*Corresponding author. E-mail: zhao@ion.chem.utk.edu.

Published on Web 05/19/2010

Scheme 1. Schematic Illustration for the Synthesis of Mixed P*t*BA/PS Brushes with a Fixed P*t*BA M_n and Various PS Molecular Weights by Sequential Atom Transfer Radical Polymerization (ATRP) and Nitroxide-Mediated Radical Polymerization (NMRP) from Y-Initiator-Functionalized Silica Particles

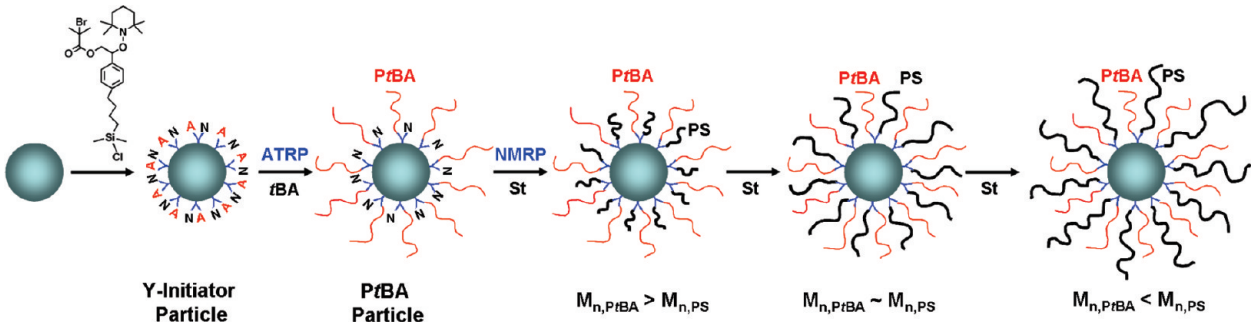

were also developed.[11−14] For example, Minko et al. reported a "grafting to" method, in which carboxyl-terminated polystyrene (PS) and poly(2-vinylpyridine) were grafted sequentially onto silicon wafers that were functionalized with 3-glycidoxypropyltrimethoxysilane.[11a] Wang et al. prepared mixed PS/poly(methyl methacrylate) brushes on silicon wafers by grafting ABC triblock copolymers with a short central B block that can form covalent bonds with silicon wafers in a one-step reaction.[11f] We reported a "grafting from" method for the synthesis of mixed brushes with controlled molecular weights, narrow polydispersities, and high grafting densities by using two different "living"/controlled radical polymerization techniques,[12a,b] atom transfer radical polymerization (ATRP) and nitroxide-mediated radical polymerization (NMRP), from asymmetric difunctional initiator (Y-initiator)-functionalized silica surfaces.[12c−f] The responsive properties of mixed brushes upon environmental variations, including solvent changes and heating, have been intensively investigated and well documented in the literature.[9−14]

Of particular interest to the present work are asymmetric mixed homopolymer brushes in which the chain lengths or grafting densities of two polymers or both are different.[2a,6,7] Here we focus on asymmetric mixed brushes that are composed of two distinct homopolymers with different molecular weights but similar grafting densities. The effect of chain length disparity on phase morphology of mixed brushes in solvents has been theoretically studied.[6,7] Using computer simulations, Roan investigated the microphase separation of immiscible mixed brushes grafted on spherical nanoparticles with a radius comparable to the polymer size $\langle R_{rms} \rangle$.[6] By varying chain lengths, grafting densities, and grafting patterns, a variety of well-ordered nanostructures can form. For example, the equilibrium nanostructure changes from rippled, to 12-islanded, and then layered with the increase of chain length disparity when the grafting densities of two polymers are identical. Wang and Müller recently used single-chain-in-mean-field simulations to study the phase behavior of asymmetric mixed brushes on flat substrates.[7] At a large chain length asymmetry, two layers can be distinguished in a solvent that is marginally good for both polymers with a slight preference for one polymer: a laterally structured bottom layer and a top layer that contains only the longer polymer species.

Asymmetric mixed brushes on planar substrates have been experimentally studied.[12d,14] Minko et al. prepared a series of asymmetric mixed brushes by a "grafting to" method and investigated them by AFM and contact angle measurements.[14] They found that for small chain length asymmetry the brushes exhibited lateral and perpendicular segregation, depending on the solvent quality. Upon increasing the molecular weight asymmetry, a transition from a "rippled" to a layered (sandwich-like) structure occurred. Using Y-initiator-functionalized silicon wafers, we synthesized mixed brushes with various chain length asymmetries and studied their responsive properties upon exposure to different solvents by AFM, XPS, and contact angle measurements.[12d] Although interesting results have been obtained from these studies, the phase morphologies of asymmetric mixed brushes have not been directly visualized.

Transmission electron microscopy (TEM) has been proven to be a powerful means for the study of phase morphologies of block copolymers in bulk and in solutions.[15] However, the use of silicon wafers as substrates for mixed brushes makes TEM studies difficult because microtoming of silicon wafers for the preparation of TEM samples is very challenging. Quite differently, silica particles can be directly used or microtomed into thin sections for visualization by TEM. Therefore, we synthesized Y-initiator-functionalized silica particles and grew mixed poly(*tert*-butyl acrylate) (P*t*BA)/PS brushes by sequential ATRP of *t*BA and NMRP of styrene.[12f] TEM studies showed that symmetric P*t*BA/PS brushes with P*t*BA M_n of 24.2 kDa and PS M_n of 23.0 kDa underwent lateral microphase separation in the melt and in nonselective solvents.[16,17] The feature sizes were on the order of $\langle R_{rms} \rangle$ values of polymers in an unperturbed state (~10 nm). In the present work, we synthesized a series of asymmetric mixed P*t*BA/PS brushes from 160 nm Y-initiator-functionalized silica particles by sequential ATRP and NMRP and studied their microphase separation behaviors in the melt after thermal annealing using differential scanning calorimetry (DSC) and TEM. P*t*BA brushes were grown first from Y-initiator particles by surface-initiated ATRP, followed by NMRP of styrene. By taking advantage of the "living" nature of NMRP,[18] mixed brushes with PS M_n smaller than, comparable to, and higher than that of P*t*BA were prepared in a one-pot reaction (Scheme 1). We note here that Motornov et al. reported the preparation of amphiphilic mixed brush-grafted particles by using a quaternization reaction between 11-bromoundodecyltrimethoxysilane-functionalized silica particles and the pyridine groups in a triblock copolymer PS-*b*-poly(2-vinylpyridine)-*b*-poly(ethylene oxide) and the responsive properties of their particles.[19]

Experimental Section

Materials. Styrene (99%, Aldrich) and *tert*-butyl acrylate (*t*-BA, 99%, Aldrich) were dried with CaH_2, distilled under a reduced pressure, and stored in a refrigerator prior to use. CuBr (98%, Aldrich) was purified according to the procedure described in the literature[20] and stored in a desiccator. *N*,*N*,*N*′,*N*′,*N*″-Pentamethyldiethylenetriamine (PMDETA, 99%, Aldrich) was dried with calcium hydride, distilled under a reduced pressure, and stored in a desiccator. Tetrahydrofuran (THF) was distilled from sodium and benzophenone and used immediately. Tetraethoxysilane (98%) and ammonium hydroxide (25% in water) were purchased from Arcos and used as received. Chlorodimethylsilane (98%) was purchased from Aldrich and used as received. The platinum−divinyltetramethyldisiloxane complex in xylene (2.1−2.4% Pt concentration in xylene) was

obtained from Gelest, Inc., and used as received. 2-[4-(But-3-enyl)phenyl]-2-(2′,2′,6′,6′-tetramethyl-1′-piperidinyloxy)ethyl 2-bromo-2-methylpropanoate (Y-initiator) was synthesized according to the procedure described in a previous publication.[12f] All other chemical reagents were purchased from either Aldrich or Fisher and used without further purification.

Characterization. Size exclusion chromatography (SEC) was carried out at ambient temperature using PL-GPC 20 (an integrated GPC system from Polymer Laboratories, Inc.) with a refractive index detector, one PLgel 5 μm guard column (50 × 7.5 mm), and two PLgel 5 μm mixed-C columns (each 300 × 7.5 mm, linear range of molecular weight from 200 to 2 000 000 according to Polymer Laboratories, Inc.). The data were processed using Cirrus GPC/SEC software (Polymer Laboratories). THF was used as the carrier solvent at a flow rate of 1.0 mL/min. Polystyrene standards (Polymer Laboratories) were used for calibration. The ^{1}H and ^{13}C NMR spectra were recorded on a Varian Mercury 300 MHz NMR spectrometer, and the residual solvent proton peak was used as the internal standard. Thermogravimetric analysis (TGA) was performed in air at a heating rate of 20 °C/min from room temperature to 800 °C using TA Q-series Q50. The hairy particle samples for TGA were dried at 50 °C in vacuum for at least 5 h.

Synthesis of 1-Phenyl-1-(2′,2′,6′,6′-tetramethyl-1′-piperidinyloxy)ethane (STEMPO). STEMPO, an initiator for nitroxide-mediated radical polymerization, was synthesized according to the procedure described in the literature.[21] ^{1}H NMR (300 MHz, $CDCl_3$) δ (ppm): 0.63 (s, CH_3, 3H), 1.00 (s, CH_3, 3H), 1.14 (s, CH_3, 3H), 1.27 (s, CH_3, 3H), 1.30−1.56 (m, 9H, CH_2 and CHCH_3), 4.75 (q, 1H, CHCH$_3$), and 7.20−7.30 (m, 5H, ArH). ^{13}C NMR ($CDCl_3$) δ (ppm): 17.20, 20.32, 23.63, 34.10, 40.30, 83.11, 126.58, 126.75, 127.99, and 145.84.

Synthesis of Bare Silica Particles. Ammonium hydroxide (25% in water, 13.860 g) and tetraethoxysilane (TEOS, 6.964 g) were dissolved separately in ethanol (each 5 mL). The solutions were added into a 500 mL flask that contained 190 mL of ethanol under stirring. The concentrations of NH_3, TEOS, and water in the solution were 0.44, 0.15, and 3.03 M, respectively. The mixture was stirred vigorously at room temperature for 6 h. The particles were isolated by centrifugation (Eppendorf 5804 centrifuge, 6000 rpm), redispersed in ethanol, and centrifugated again. This washing process was repeated with ethanol one more time, water four times, and ethanol again. Particles were then dried with a stream of air flow (2.261 g). The average size of particles was 160 nm, determined by TEM image analysis.

Synthesis of Y-Initiator-Functionalized Silica Particles. 2-[4-(But-3-enyl)phenyl]-2-(2′,2′,6′,6′-tetramethyl-1′-piperidinyloxy)ethyl 2-bromo-2-methylpropanoate (Y-initiator, 0.261 g, 0.545 mmol) was added into a 25 mL two-necked flask and dried at room temperature in vacuum for 30 min. Chlorodimethylsilane (2.0 mL, 18.4 mmol) was injected via a disposable syringe into the flask under a N_2 atmosphere, followed by addition of Pt complex in xylene (15 μL). The mixture was stirred under a nitrogen atmosphere at room temperature, and the hydrosilylation reaction was monitored by ^{1}H NMR spectroscopy analysis. Once the reaction was complete, excess chlorodimethylsilane was removed by vacuum and the product (Y-silane) was used directly in the next step for the preparation of Y-initiator-functionalized silica particles.

Silica particles (1.081 g) were dried at 110 °C in vacuum (~30 mTorr) for 6−7 h and were dispersed in dry THF (10 mL). A solution of Y-silane freshly synthesized from 0.261 g of Y initiator in dry THF (2 mL) was injected into the dispersion via a syringe. The mixture was stirred at 70 °C under a N_2 atmosphere for 49 h. The particles were then isolated by centrifugation, redispersed in THF, and centrifugated again. This washing process was repeated four times, followed by drying with a stream of air flow to yield dry particles (0.853 g).

Synthesis of Poly(*tert*-butyl acrylate) (P*t*BA) Brush-Grafted Silica Particles. Y-initiator-functionalized silica particles (Y-initiator particles, 0.406 g) and anisole (9.888 g) were added into a 50 mL two-necked flask. The mixture was ultrasonicated in an ultrasonic water bath to form a stable dispersion. CuBr (53.9 mg, 0.374 mmol), *tert*-butyl acrylate (*t*BA, 19.37 g, 151.3 mmol), *N*,*N*,*N*′,*N*′,*N*″-pentamethyldiethylenetriamine (PMDETA, 65.9 mg, 0.380 mmol), and ethyl 2-bromoisobutyrate (EBiB, 48.6 mg, 0.249 mmol) were added into a separate 100 mL three-necked flask and stirred under a N_2 atmosphere. The particle dispersion was then transferred into the three-necked flask via a syringe, and the reaction mixture was degassed by three freeze−pump−thaw cycles. The flask was placed in an oil bath with a preset temperature of 75 °C, and the polymerization was monitored by SEC and ^{1}H NMR spectroscopy analysis. After the reaction proceeded for 38 h, the flask was removed from the oil bath and opened to air. THF (20 mL) was added into the flask to dilute the mixture. The particles were separated by centrifugation, and the supernatant was passed through a column of neutral, activated aluminum oxide to remove the copper catalyst. The particles were redispersed in THF, allowed to stand at ambient conditions for 2 h (the green precipitate was removed), and centrifugated again. This washing process was repeated with THF one more time and chloroform three times, followed by drying the particles with a stream of air flow, yielding P*t*BA brush-grafted silica particles (0.405 g). The $M_{n,SEC}$ and polydispersity index (PDI) of the free P*t*BA formed from the free initiator in the polymerization were 24.5 kDa and 1.11, respectively, determined from SEC analysis using polystyrene calibration.

Synthesis of Mixed P*t*BA/PS Brush-Grafted Silica Particles. The P*t*BA brush-grafted silica particles (0.342 g) were dispersed in anisole (18.218 g) in a 50 mL two-necked flask using an ultrasonic water bath. The particle dispersion was then transferred into a 100 mL three-necked flask that contained free NMRP initiator STEMPO (65.4 mg, 0.251 mmol), followed by the addition of styrene (26.016 g, 250.2 mmol). The mixture was degassed by three freeze−pump−thaw cycles. The flask was then placed in a 120 °C oil bath, and the polymerization was monitored by ^{1}H NMR spectroscopy and SEC analysis. Samples were taken from the reaction mixture using a degassed syringe when the molecular weight of the free polystyrene formed from the free initiator reached desired values. The samples were diluted with THF. The particles were separated from the free polymer by centrifugation, redispersed in THF, and centrifugated again. For each sample, this washing process was repeated four times to remove the physically adsorbed polymer. The particles were then dried with a stream of air flow.

Differential Scanning Calorimetry (DSC) Study of P*t*BA Brush- and Mixed P*t*BA/PS Brush-Grafted Silica Particles. DSC analysis of polymer brush-grafted particles was conducted on a TA Q-1000 DSC instrument that was calibrated with the sapphire standard. The hairy particles were thermally annealed at 120 °C in vacuum for 3 h and then cooled to room temperature. For each sample, approximately 10−15 mg of particles was used in the analysis. The heating and cooling rates were 10 °C/min; the second heating thermogram was used to determine the glass transitions.

Transmission Electron Microscopy (TEM) Study. Chloroform, a good solvent for both P*t*BA and PS, was used to prepare the particle dispersions. For each sample, about 1 mg of particles was dispersed in 2 mL of chloroform in a vial by ultrasonication for 5 min. A drop of the particle dispersion was cast onto a carbon-coated mica and allowed to dry at ambient temperature. The sample-loaded carbon films on mica were floated onto the surface of double-distilled water in a crystallization dish and picked up with 400-mesh copper grids. The samples were thermally annealed in vacuum at 120 °C for 3 h and then stained with RuO_4 vapor at room temperature for 30 min. TEM experiments were performed on a JEOL 1200EX at an accelerating voltage of 80 kV. The images were analyzed using the Image Processing Tool Kit 2.5 software (Reindeer, Inc.).

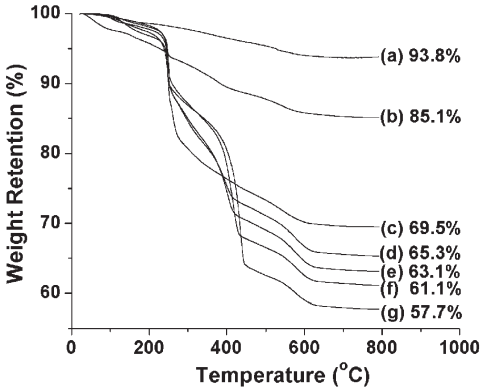

Figure 1. Thermogravimetric analysis (TGA) of (a) bare particles, (b) Y-initiator particles, (c) P*t*BA brush-grafted particles, (d) mixed brush-grafted particles with P*t*BA $M_{n,SEC}$ of 24.5 kDa and PS M_n of 14.8 kDa (particle **1**), (e) mixed brush-grafted particles with P*t*BA $M_{n,SEC}$ of 24.5 kDa and PS M_n of 18.7 kDa (particle **2**), (f) mixed brush-grafted particles with P*t*BA $M_{n,SEC}$ of 24.5 kDa and PS M_n of 24.9 kDa (particle **3**), and (g) mixed brush-grafted particles with P*t*BA $M_{n,SEC}$ of 24.5 kDa and PS M_n of 30.4 kDa (particle **4**). TGA was performed in air at a heating rate of 20 °C/min from room temperature to 800 °C.

Results and Discussion

Synthesis of Mixed P*t*BA/PS Brushes on Silica Particles with a Fixed P*t*BA M_n and Various PS Molecular Weights. The Y-initiator-functionalized silica particles were prepared via a procedure that we reported before using the Y-initiator-terminated monochlorosilane (Y-silane) and 160 nm bare silica particles.[12f] The bare silica particles were synthesized by the Stöber process, which involves the hydrolysis and condensation of tetraethoxysilane in an ammonia/ethanol solution and is known to produce silica particles with a relatively uniform size distribution.[22] Thermogravimetric analysis (TGA) showed that the weight loss of Y-initiator particles relative to bare silica particles was comparable to our previous result if the difference at 100 °C between the two curves was taken into consideration (Figure 1).[12f]

The Y-initiator particles were then used for preparing mixed P*t*BA/PS brush samples. The surface-initiated ATRP of *tert*-butyl acrylate from Y-initiator particles was carried out in anisole at 75 °C using CuBr/PMDETA as catalyst in the presence of a free initiator, ethyl 2-bromoisobutyrate (EBiB). We confirmed before that the TEMPO group in the Y-initiator was stable under this ATRP condition.[12] The addition of a free initiator to the polymerization mixture not only made it possible to control the surface-initiated polymerization by the solution polymerization but also allowed us to conveniently monitor the polymerization by ^{1}H NMR spectroscopy and SEC analysis. We found that the $M_{n,SEC}$ and PDI of free P*t*BA were 14.1 kDa and 1.13, respectively, at polymerization time of 16 h, 19.6 kDa and 1.10, respectively, at 24 h, and 24.5 kDa and 1.11, respectively, at 38 h, indicating that the reaction was a controlled process. The polymerization was stopped at the monomer conversion of 31.4%, which corresponded to a degree of polymerization (DP) of P*t*BA of 191. The P*t*BA brush-grafted particles were isolated by centrifugation and repeatedly washed with THF and $CHCl_3$ to remove the physically adsorbed free polymer. The $M_{n,SEC}$ and PDI of the free P*t*BA formed from the free initiator EBiB were 24.5 kDa and 1.11, respectively, determined by SEC using polystyrene standards. TGA showed that the weight retention of P*t*BA brush-grafted silica particles at 800 °C was 69.5%. We and other researchers confirmed that the molecular weight and molecular weight distribution of polymer brushes synthesized by "living"/controlled radical polymerization were essentially identical to those of the free polymer formed from the free initiator.[12f,23] By using the average size of bare silica particles, TGA data, and the DP of free P*t*BA, and assuming that the density of silica particles was identical to bulk SiO_2 (2.07 g/cm^3), the grafting density of P*t*BA brushes on silica particles was calculated to be 2.8 nm^2/chain or 0.36 chains/nm^2. This value was very close to that of P*t*BA brushes on 180 nm silica particles reported before.[12f]

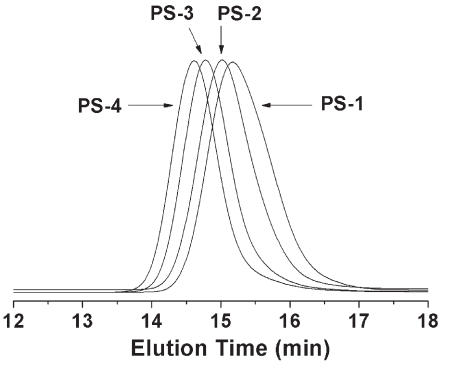

Figure 2. Size exclusion chromatography traces of four polymers formed from free initiator STEMPO at different polymerization times in the synthesis of mixed P*t*BA/PS brush-grafted silica particles by NMRP of styrene at 120 °C from P*t*BA brush-grafted particles.

Mixed P*t*BA/PS brush-grafted particles were obtained after the surface-initiated NMRP of styrene from the P*t*BA brush-grafted particles. Again, a free initiator, 1-phenyl-1-(2′,2′,6′,6′-tetramethyl-1′-piperidinyloxy)ethane (STEMPO), was added into the reaction mixture. The polymerization was carried out at 120 °C and monitored by SEC. Four samples with different PS molecular weights were taken from the reaction mixture at different polymerization times. The hairy particles were isolated by centrifugation and repeatedly washed with THF. The free polymers were precipitated in methanol and analyzed by SEC. Note that the C−Br bond at the grafted P*t*BA chain end is relatively weak and might participate in the chain transfer process in the NMRP of styrene. We previously used tri(*n*-butyl)tin hydride to remove the bromine atom from the P*t*BA chain end;[12f] however, it was nontrivial to completely remove the tin compound, and any tin residue could interfere with the NMRP of styrene. In the synthesis of block copolymers from asymmetric difunctional initiators by combining ATRP and NMRP, Tunca et al. did not remove the bromine atom from the polymer chain end but used the polymer directly for the preparation of block copolymers by NMRP,[24] suggesting that the possible chain transfer to the P*t*BA chain end in the NMRP of styrene was negligible. In this work, we synthesized mixed P*t*BA/PS brushes by surface-initiated NMRP of styrene from P*t*BA brush-grafted particles without dehalogenation.

Figure 2 shows the SEC traces of four polymers taken at different polymerization times. The M_n of PS increased from 14.8 kDa (PS-**1**; the corresponding mixed P*t*BA/PS brush-grafted particle sample designated as particle **1**), to 18.7 kDa (PS-**2**; the corresponding mixed P*t*BA/PS brush-grafted particle sample designated as particle **2**), to 24.9 kDa (PS-**3**; the corresponding mixed P*t*BA/PS brush-grafted particle sample designated as particle **3**), and 30.4 kDa (PS-**4**; the corresponding mixed P*t*BA/PS brush-grafted particle sample designated as particle **4**), while the PDI remained narrow (< 1.25). From Figure 1, the weight retention of mixed brush-grafted particles at 800 °C decreased with the increase of PS M_n, from 65.3% for particle **1**, to 63.1% for particle **2**, to 61.1% for particle **3**, and 57.7% for

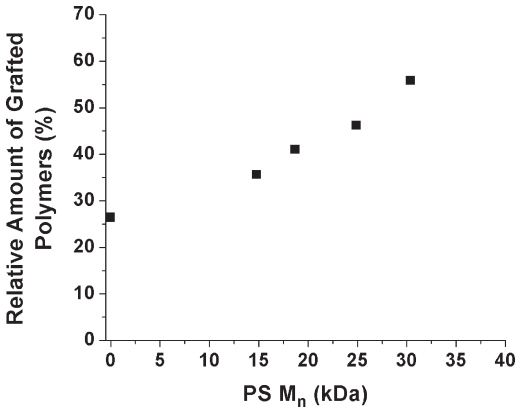

Figure 3. Amount of the grafted polymers relative to the silica residue calculated from TGA data versus polystyrene molecular weight.

particle **4**. If the residue (silica) at 800 °C is used as reference, the amount of the polymers grafted on silica particles can be calculated. Figure 3 shows the relative mass of the grafted polymers versus the molecular weight of PS; the amount of the grafted polymers increased with PS M_n in a nearly linear fashion, indicating that the polymerization was controlled.

On the basis of the size of bare silica particles, TGA data, and PS molecular weight, the grafting density of PS for each sample was calculated. The results are summarized in Table 1. The grafting densities of two polymers in these samples were reasonably close to each other. Calculations showed that the average distance between grafting sites in these mixed brushes was 1.2−1.3 nm, indicating that the polymers were densely grafted. To confirm that the tethered polymers were in the brush regime, we estimated the radii of gyration ($\langle R_g \rangle$) of free polymers having the same molecular weights in their unperturbed states[25] and found that they were more than twice larger than the average distance between the grafting points (see Table 1). According to the results from Cheng et al.,[26] when the reduced tethering density, defined as $\sigma\pi R_g^2$ (where σ is the reciprocal of the cross-sectional area per chain and R_g is the radius of gyration of the free polymer), is greater than 14.3, the grafted polymer chains are in the highly stretched brush regime. If the reduced tethering density is between 3.7 and 14.3, the tethered chains are in the crossover zone between the polymer mushroom and highly stretched polymer brush regimes. Calculations show that the reduced total grafting densities of four mixed P*t*BA/PS brush samples were >23 (the average of the $\langle R_g \rangle$ values of the two polymers in each sample was used in the calculation), which further confirmed that the grafted polymers in these samples were in the highly stretched brush regime.

DSC Study of Mixed P*t*BA/PS Brush-Grafted Silica Particles with a Fixed P*t*BA M_n and Various PS Molecular Weights. We previously observed that for microphase-separated mixed P*t*BA/PS brushes on silica particles two glass transitions appeared in the DSC thermogram, while miscible mixed brushes exhibited only one broad glass transition.[16] This observation evidences that DSC is a powerful means to determine whether the two grafted polymers in the brush layer microphase separate or not. Therefore, we performed DSC analysis of all four mixed brush-grafted particle samples. For comparison, P*t*BA brush-grafted particles were also studied. Prior to the analysis, the particles were thermally annealed at 120 °C in vacuum for 3 h and then cooled in vacuum to room temperature. The results from DSC studies are shown in Figure 4. The glass transition of P*t*BA homopolymer brushes on silica particles occurred at 45 °C

Table 1. Molecular Characteristics of Mixed P*t*BA/PS Brushes with a Fixed P*t*BA $M_{n,SEC}$ of 24.5 kDa and Various PS Molecular Weights on 160 nm Silica Particles and the Corresponding Free Polymers[a]

sample	PS M_n (Da), PDI, and DP[b]	σ_{PS} and σ_{total} (chains/nm^2)[c]	$\langle R_{rms} \rangle$ and $\langle R_g \rangle$ (nm)[d]
particle **1**	14 800, 1.24, 142	0.21, 0.57	8.0, 3.3
particle **2**	18 700, 1.20, 180	0.26, 0.62	9.0, 3.7
particle **3**	24 900, 1.17, 239	0.27, 0.63	10.4, 4.2
particle **4**	30 400, 1.14, 292	0.32, 0.68	11.5, 4.7

[a] The $M_{n,SEC}$ and PDI of P*t*BA were 24.5 kDa and 1.11, respectively, determined by SEC using PS calibration; the degree of polymerization (DP) of P*t*BA was 191, calculated by using the monomer conversion and the monomer-to-initiator ratio; the grafting density of P*t*BA (σ_{PtBA}) was 0.36 chains/nm^2, calculated by using the DP of P*t*BA, TGA data, and the average size of bare silica particles (160 nm). [b] The M_ns and the values of polydispersity index (PDI) of polystyrenes were determined by SEC using PS standards; the DPs of polystyrenes were calculated from M_ns. [c] The polystyrene grafting density (σ_{PS}) in each sample was calculated based on the size of bare particles (160 nm), DP of free polystyrene, and TGA data along with the assumptions that the particles were spherical and the silica particle density was 2.07 g/cm^3. The total grafting density $\sigma_{total} = \sigma_{PtBA} + \sigma_{PS}$. [d] $\langle R_{rms} \rangle$ and $\langle R_g \rangle$ are root-mean-square end-to-end distance (nm) and radius of gyration (nm) of polymer chains in an unperturbed state, respectively. The values of $\langle R_{rms} \rangle$ were calculated by using $\langle R_{rms} \rangle = (C_\infty nl^2)^{1/2}$, where C_∞ is the Flory's characteristic ratio for an infinite chain, n the number of C−C bonds in the chain (n = 2DP), and l the bond length of C−C bond (1.54 Å).[25] The values of $\langle R_g \rangle$ were calculated by using $\langle R_g \rangle = (\langle R_{rms} \rangle^2/6)^{1/2}$. The value of C_∞ for P*t*BA was not available in the literature. We used the value of C_∞ of PS in the calculation of the $\langle R_{rms} \rangle$ value of P*t*BA. The calculated values of $\langle R_{rms} \rangle$ and $\langle R_g \rangle$ of P*t*BA with a DP of 191 in the unperturbed state were 9.3 and 3.8 nm, respectively.

(thermogram **1**), which was about 10 °C higher than the T_g of free P*t*BA with a similar molecular weight,[16] consistent with our previous observation. This is believed to be the result of surface tethering effect. Savin et al. also observed an increase in the T_g of homopolymer brushes grafted on silica nanoparticles compared with the corresponding free polymer.[27] All four mixed P*t*BA/PS brush-grafted particle samples exhibited two distinct glass transitions with the middle points being located at ∼47 and ∼90 °C (thermograms **2**, **3**, **4**, and **5**). These two transitions corresponded to the glass transitions of P*t*BA and PS, respectively, suggesting that the two grafted polymers phase separated into separate microdomains that consisted of nearly pure polymer species. Since one end of the polymer chains was fixed via a covalent bond on the surface of silica particles, the microphase separation was confined in the brush layer.

A closer examination of thermograms of mixed brush-grafted particles in Figure 4 revealed that with the increase of PS molecular weight the magnitude and width of PS glass transition increased (using the P*t*BA glass transition as reference). In particular, the glass transition of PS in particle **4** occurred over a temperature range of 20 °C (thermogram **5**), which could be due to the fact that the chain length of PS (DP = 292) was substantially longer than that of P*t*BA (DP = 191). As suggested by simulation studies,[7] it is very likely that the P*t*BA chains and the inner part of PS chains undergoes lateral microphase separation in the bottom layer, while the outer part of PS chains forms a thin layer that covers the microphase-separated microdomains of PS and P*t*BA. The broad glass transition could be the result of different mobilities of PS segments in the two layers. Interestingly, with the increase of PS M_n from 14.8, to 18.7, to 24.9, and 30.4 kDa, the glass transition temperatures of both polymers shifted to slightly higher values. While the increase of P*t*BA T_g was quite small (1−2 °C), the middle point of the PS T_g increased noticeably from 88, to 90, to 93, and 94 °C,

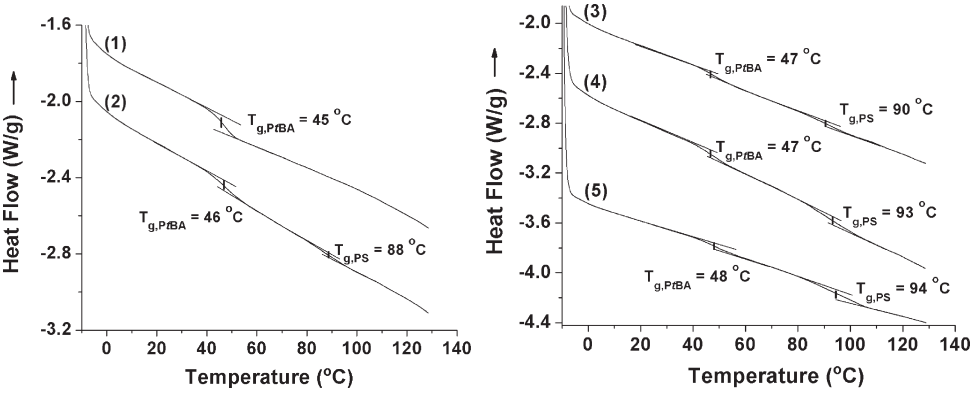

Figure 4. Differential scanning calorimetry (DSC) analysis of (1) P*t*BA brush-grafted silica particles (P*t*BA $M_{n,SEC}$ = 24.5 kDa), (2) particle **1** (P*t*BA $M_{n,SEC}$ = 24.5 kDa and PS M_n = 14.8 kDa), (3) particle **2** (P*t*BA $M_{n,SEC}$ = 24.5 kDa and PS M_n = 18.7 kDa), (4) particle **3** (P*t*BA $M_{n,SEC}$ = 24.5 kDa and PS M_n = 24.9 kDa), and (5) particle **4** (P*t*BA $M_{n,SEC}$ = 24.5 kDa and PS M_n = 30.4 kDa). The heating and cooling rates in the DSC analysis were 20 °C/min.

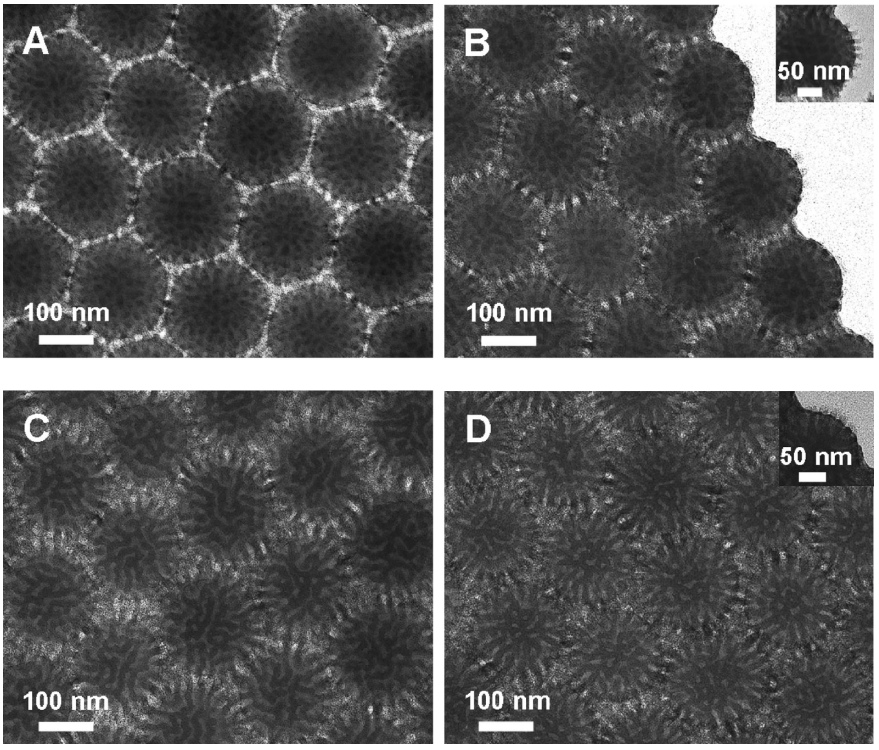

Figure 5. Top-view TEM micrographs of (A) particle **1** (P*t*BA $M_{n,SEC}$ = 24.5 kDa, PS M_n = 14.8 kDa), (B) particle **2** (P*t*BA $M_{n,SEC}$ = 24.5 kDa, PS M_n = 18.7 kDa), (C) particle **3** (P*t*BA $M_{n,SEC}$ = 24.5 kDa, PS M_n = 24.9 kDa), and (D) particle **4** (P*t*BA $M_{n,SEC}$ = 24.5 kDa, PS M_n = 30.4 kDa) after being cast from $CHCl_3$, a nonselective good solvent for both P*t*BA and PS, and thermally annealed at 120 °C in vacuum for 3 h. The samples were stained with RuO_4 vapor.

which might be due to the molecular weight effect on T_g. It is known that the glass transition temperature is higher when the polymer molecular weight is higher before a plateau value is reached.[25] In summary, for all four mixed brush samples, two distinct glass transitions were observed from DSC analysis, implying that the two grafted polymers phase separated in the brush layer.

TEM Study of Mixed P*t*BA/PS Brushes on Silica Particles with P*t*BA $M_{n,SEC}$ of 24.5 kDa and PS M_n Varying from 14.8 to 30.4 kDa. To prepare samples for the TEM study, the mixed brush-grafted particles were dispersed in $CHCl_3$, a nonselective good solvent for both P*t*BA and PS, and drop-cast onto carbon films. After the solvent was evaporated, the samples were thermally annealed at 120 °C in vacuum for 3 h and then stained with RuO_4 vapor at room temperature for 30 min. Figure 5 shows the typical top-view TEM micrographs of four mixed brush particle samples. Note that RuO_4 selectively stains PS chains, making PS and P*t*BA microdomains

Scheme 2. Schematic Illustration of Phase Morphologies of Mixed P*t*BA/PS Brushes with a Fixed P*t*BA Molecular Weight and Varying PS Molecular Weight

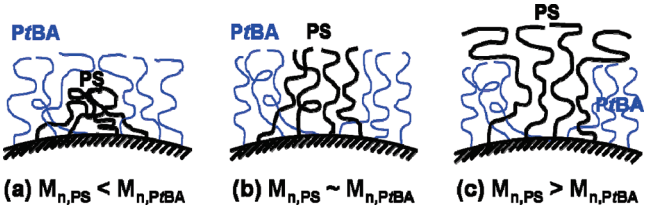

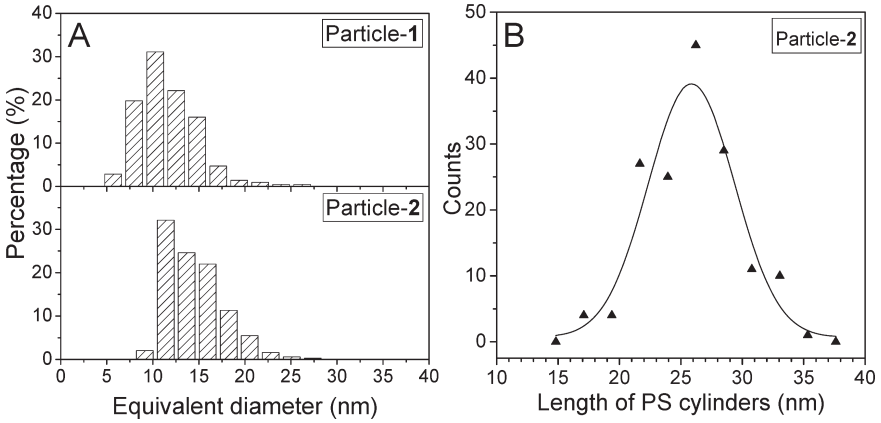

Figure 6. Equivalent diameter distributions (A) of polystyrene nanodomains in particle **1** (P*t*BA $M_{n,SEC}$ = 24.5 kDa, PS M_n = 14.8 kDa) and particle **2** (P*t*BA $M_{n,SEC}$ = 24.5 kDa, PS M_n = 18.7 kDa) and cylinder length distribution (B) of PS nanodomains in particle **2** from TEM image analysis. A Gaussian function was used to fit the statistical data in order to guide eyes.

appear dark and bright, respectively. By quickly looking through the four TEM images, one can easily find out that the phase morphology of mixed P*t*BA/PS brushes grafted on silica particles changes with the molecular weight of PS. For particle **1** in which the molecular weight of PS (14.8 kDa) was substantially smaller than that of P*t*BA (24.5 kDa), relatively short PS chains segregated into isolated, nearly spherical microdomains (Figure 5A). A distinctive feature of Figure 5A is that the silica particles were separated from each other by a bright gap that was filled with "invisible" (i.e., unstained) P*t*BA chains, though occasionally dark PS nanodomains were found to bridge neighboring particles. Thus, it was very likely that PS microdomains were buried inside the P*t*BA matrix (Scheme 2a).

The size of PS nanodomains was retrieved from TEM image analysis using Image Processing Tool Kit 2.5 software. We were aware that TEM only showed a two-dimensional projection image of mixed brush features on spherical SiO_2 particles. However, restoring the three-dimensional (3D) image from a 2D image was nontrivial, and we had to ignore the 3D effect on the actual feature sizes in our image analysis. To minimize errors, we purposely chose areas in the center of spherical particles for the analysis of feature size. The average equivalent diameter of PS microdomains in Figure 5A was 11.5 nm (Figure 6A). Note that the $\langle R_{rms} \rangle$ of PS with a molecular weight of 14.8 kDa in the unperturbed state was 8.0 nm, reasonably comparable to the equivalent diameter. With the increase of PS molecular weight to 18.7 kDa, the isolated PS nanodomains began to merge into short cylinders but did not fully connect (Figure 5B), though the PS chain length (DP = 180) was quite close to that of P*t*BA (DP = 191). This is likely because the PS grafting density (0.26 chains/nm^2) is slightly lower than that of P*t*BA (0.36 chains/nm^2). A calculation shows that the volume ratio of P*t*BA to PS is 65:35;[28] an immiscible diblock copolymer with such a volume ratio for the two blocks is most likely to exhibit a cylindrical phase.[29] The grafted polymer chains spread out and covered the interstitials of particles. Moreover, some dark domains formed bridges among neighboring particles. From the edge of the hairy particle shown in the inset of Figure 5B, both dark and bright nanodomains appeared to be present at the brush−vacuum interface. Note that the surface free energies of P*t*BA and PS are close to each other.[30,31] The average equivalent diameter and cylinder length of PS microdomains from the image analysis were 14.5 and 26.0 nm, respectively (Figure 6).

For particle **3** in which the P*t*BA $M_{n,SEC}$ was 24.5 kDa and the PS M_n was 24.9 kDa (the grafting densities of P*t*BA and PS were 0.36 and 0.27 chains/nm^2, respectively), a nearly bicontinuous, random wormlike morphology was observed, which is the same as the phase separated nanostructure of mixed P*t*BA/PS brushes with P*t*BA $M_{n,SEC}$ of 24.2 kDa and PS M_n of 23.0 kDa on 180 nm silica particles that we reported before (Scheme 2b)[17] and is similar to the results obtained from computer simulations by Wang and Müller.[7] Again, the grafted polymer chains were highly stretched and spread out; the interstitials among silica particles were completely covered by the phase-separated PS and P*t*BA chains. Some dark PS and bright P*t*BA stripes bridged among neighboring particles. From the image analysis, the widths of PS and P*t*BA stripes were 14.0 and 12.3 nm, respectively. The distributions of the widths of PS and P*t*BA microdomains are shown in Figure 7. Note that the values of $\langle R_{rms} \rangle$ of the corresponding free PS and P*t*BA in the unperturbed states were 10.4 and 9.3 nm, respectively. Our results again corroborate the theoretical prediction that the ripple wavelength is about twice the $\langle R_{rms} \rangle$ of polymers. It should be noted here that for this sample the DPs of P*t*BA and PS were not identical but 191 and 239, respectively. Computer simulation studies have shown that the bicontinuous "rippled" nanostructure can tolerate small chain length asymmetries.[6,7]

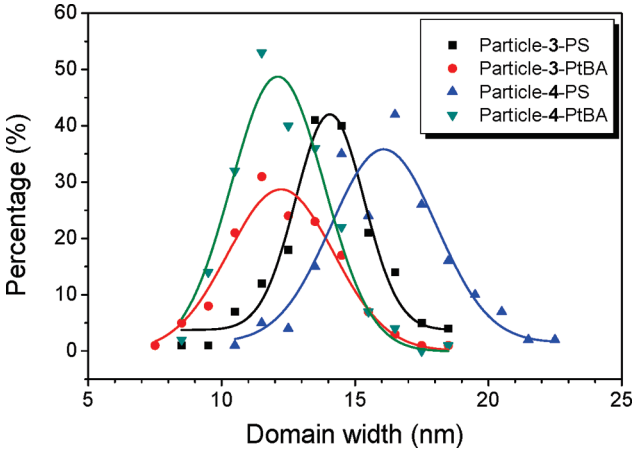

Figure 7. Width distributions of PS and P*t*BA microdomains in particle **3** (P*t*BA $M_{n,SEC}$ = 24.5 kDa, PS M_n = 24.9 kDa) and particle **4** (P*t*BA $M_{n,SEC}$ = 24.5 kDa, PS M_n = 30.4 kDa) from the TEM image analysis. A Gaussian function was used to fit the statistical data in order to guide eyes.

Figure 5D shows a typical micrograph of particle **4** in which the P*t*BA $M_{n,SEC}$ (24.5 kDa) was lower than that of PS

M_n (30.4 kDa) and the grafting densities of P*t*BA and PS were 0.36 and 0.32 chains/nm^2, respectively. Compared with the image in Figure 5C, a morphology transition can be seen; bridges that connected the dark PS stripes began to form, and more bright P*t*BA domains became isolated. Unlike the PS nanodomains in Figure 5A, the shape of the P*t*BA nanodomains here appeared to be more irregular. An examination of the interstitials among silica particles and the edge of the hairy particle (the inset in Figure 5D) suggested that the isolated P*t*BA nanodomains were buried in the continuous PS matrix (Scheme 2c), which can be explained by the fact that the grafting densities of P*t*BA and PS were very close to each other and the chain length of PS (DP = 292) was longer by 101 than that of P*t*BA (DP = 191). This observation is consistent with the prediction for asymmetric mixed brushes that at a large chain length asymmetry a two-layered structure is formed in which the bottom layer is laterally microphase separated and covered by the longer polymer species that form the upper layer.[7] A quantitative analysis shows that the width of PS domains increased slightly from 14.0 nm in particle **3** to 16.2 nm for particle **4** (Figure 7), while the width of P*t*BA nanodomains remained the same, i.e., 12.3 nm. Thus, our TEM studies evidently showed that when the P*t*BA chain length was fixed, the phase morphology of mixed P*t*BA/PS brushes changed from the isolated PS nanodomains in the P*t*BA matrix at a relatively low DP of PS, to bicontinuous wormlike nanostructures at the PS chain length slightly higher but comparable to that of P*t*BA, and to a two-layer structure in which the bottom layer was laterally phase-separated and covered by a thin PS layer at the PS M_n much higher than that of P*t*BA. Note that we cannot rule out the contribution of the slight difference in the grafting densities of two polymers in the first three samples, but the morphology evolution appears to be mainly governed by the chain length disparity.

Conclusions

We synthesized a series of mixed P*t*BA/PS brushes with a fixed P*t*BA $M_{n,SEC}$ of 24.5 kDa and the PS M_n varying from 14.8, to 18.7, to 24.9, and to 30.4 kDa on 160 nm Y-initiator-functionalized silica particles by combining ATRP and NMRP. Based on the TGA data, the size of silica particles, and the DPs of free polymers, the grafting densities of two polymers in these samples were calculated and found to be comparable to each other. Two distinct glass transitions, located at ~47 and ~90 °C, were observed from DSC analysis for all four mixed brush particle samples, suggesting that the two grafted polymers underwent microphase separation. TEM studies evidently showed that the phase morphology of mixed brushes on silica particles evolved from isolated PS nanodomains in the P*t*BA matrix, to bicontinuous, random wormlike nanostructures, and to a two-layer structure in which the bottom layer was laterally phase-separated and covered by the longer polymer chains with the increase of PS molecular weight from below to above that of P*t*BA. This is the first time that the theoretically predicted morphology evolution of mixed brushes with the change of chain length disparity between two grafted polymers was directly observed from TEM. The results reported in this article could open up new opportunities in the preparation of novel nanostructured hairy particles and the applications of mixed homopolymer brushes in technological uses.

Acknowledgment. B.Z. thanks the University of Tennessee and NSF (DMR-0906913 and -1007986) for the support of this work. G.Z. thanks the Chinese Scholar Council for financial support.

References and Notes

(1) (a) Marko, J. F.; Witten, T. A. *Phys. Rev. Lett.* **1991**, *66*, 1541–1544. (b) Marko, J. F.; Witten, T. A. *Macromolecules* **1992**, *25*, 296–307. (c) Dong, H. *J. Phys. II* **1993**, *3*, 999–1020. (d) Brown, G.; Chakrabarti, A.; Marko, J. F. *Europhys. Lett.* **1994**, *25*, 239–244. (e) Luzinov, I.; Minko, S.; Tsukruk, V. V. *Prog. Polym. Sci.* **2004**, *29*, 635–698. (f) Luzinov, I.; Minko, S.; Tsukruk, V. V. *Soft Matter* **2008**, *4*, 714–725. (g) Zhao, B.; Brittain, W. J. *Prog. Polym. Sci.* **2000**, *25*, 677–710.

(2) (a) Lai, P. Y. *J. Chem. Phys.* **1994**, *100*, 3351–3357. (b) Soga, K. G.; Zuckermann, M. J.; Guo, H. *Macromolecules* **1996**, *29*, 1998–2005. (c) Zhulina, E.; Balazs, A. C. *Macromolecules* **1996**, *29*, 2667–2673. (d) Singh, C.; Pickett, G. T.; Balazs, A. C. *Macromolecules* **1996**, *29*, 7559–7570. (e) Müller, M. *Phys. Rev. E* **2002**, *65*, 030802. (f) Minko, S.; Müller, M.; Usov, D.; Scholl, A.; Froeck, C.; Stamm, M. *Phys. Rev. Lett.* **2002**, *88*, 035502. (g) Wenning, L.; Müller, M.; Binder, K. *Europhys. Lett.* **2005**, *71*, 639–645.

(3) Zhao, B.; Zhu, L. *Macromolecules* **2009**, *42*, 9369–9383.

(4) (a) Zhu, M.-Q.; Wang, L.-Q.; Exarhos, G. J.; Li, A. D. Q. *J. Am. Chem. Soc.* **2004**, *126*, 2656–2657. (b) Li, D. J.; Jones, G. L.; Dunlap, J. R.; Hua, F. J.; Zhao, B. *Langmuir* **2006**, *22*, 3344–3351. (c) Li, D. J.; Zhao, B. *Langmuir* **2007**, *23*, 2208–2217. (d) Li, D. J.; Dunlap, J. R.; Zhao, B. *Langmuir* **2008**, *24*, 5911–5918. (e) Jiang, X. M.; Wang, B. B.; Li, C. Y.; Zhao, B. *J. Polym. Sci., Part A: Polym. Chem.* **2009**, *47*, 2853–2870. (f) Wu, T.; Zou, G.; Hu, J.; Liu, S. *Chem. Mater.* **2009**, *21*, 3788–3798.

(5) Boyer, C.; Whittaker, M. R.; Luzon, M.; Davis, T. P. *Macromolecules* **2009**, *42*, 6917–6926.

(6) Roan, J.-R. *Phys. Rev. Lett.* **2006**, *96*, 248301.

(7) Wang, J.; Müller, M. *J. Phys. Chem. B* **2009**, *113*, 11384–11402.

(8) Merlitz, H.; He, G. L.; Sommer, J. U.; Wu, C. X. *Macromolecules* **2009**, *42*, 445–451.

(9) Sidorenko, A.; Minko, S.; Schenk-Meuser, K.; Duschner, H.; Stamm, M. *Langmuir* **1999**, *15*, 8349–8355.

(10) (a) Minko, S.; Usov, D.; Goreshnik, E.; Stamm, M. *Macromol. Rapid Commun.* **2001**, *22*, 206–211. (b) Motornov, M.; Minko, S.; Eichhorn, K. J.; Nitschke, M.; Simon, F.; Stamm, M. *Langmuir* **2003**, *19*, 8077–8085. (c) Lemieux, M.; Usov, D.; Minko, S.; Stamm, M.; Shulha, H.; Tsukruk, V. V. *Macromolecules* **2003**, *36*, 7244–7255. (d) Usov, D.; Gruzdev, V.; Nitschke, M.; Stamm, M.; Hoy, O.; Luzinov, I.; Tokarev, I.; Minko, S. *Macromolecules* **2007**, *40*, 8774–8783. (e) Santer, S.; Kopyshev, A.; Yang, H. K.; Rühe, J. *Macromolecules* **2006**, *39*, 3056–3064.

(11) (a) Minko, S.; Patil, S.; Datsyuk, V.; Simon, F.; Eichhorn, K. J.; Motornov, M.; Usov, D.; Tokarev, I.; Stamm, M. *Langmuir* **2002**, *18*, 289–296. (b) Minko, S.; Müller, M.; Motornov, M.; Nitschke, M.; Grundke, K.; Stamm, M. *J. Am. Chem. Soc.* **2003**, *125*, 3896–3900. (c) Ionov, L.; Minko, S.; Stamm, M.; Gohy, J. F.; Jerome, R.; Scholl, A. *J. Am. Chem. Soc.* **2003**, *125*, 8302–8306. (d) Ionov, L.; Sidorenko, A.; Stamm, M.; Minko, S.; Zdyrko, B.; Klep, V.; Luzinov, I. *Macromolecules* **2004**, *37*, 7421–7423. (e) LeMieux, M. C.; Julthongpiput, D.; Bergman, K. N.; Cuong, P. D.; Ahn, H. S.; Lin, Y. H.; Tsukruk, V. V. *Langmuir* **2004**, *20*, 10046–10054. (f) Wang, J.; Kara, S.; Long, T. E.; Ward, T. C. *J. Polym. Sci., Polym. Chem.* **2000**, *38*, 3742–3750. (g) Julthongpiput, D.; Lin, Y. H.; Teng, J.; Zubarev, E. R.; Tsukruk, V. V. *Langmuir* **2003**, *19*, 7832–7836. (h) Tsujii, Y.; Ohno, K.; Yamamoto, S.; Goto, A.; Fukuda, T. *Adv. Polym. Sci.* **2006**, *197*, 1–45. (i) Ionov, L.; Houbenov, N.; Sidorenko, A.; Stamm, M.; Luzinov, I.; Minko, S. *Langmuir* **2004**, *20*, 9916–9919. (j) Ionov, L.; Sidorenko, A.; Stamm, M.; Minko, S.; Zdyrko, B.; Klep, V.; Luzinov, I. *Macromolecules* **2004**, *37*, 7421–7423. (k) Motornov, M.; Sheparovych, R.; Tokarev, I.; Roiter, Y.; Minko, S. *Langmuir* **2007**, *23*, 13–19. (l) Sheparovych, R.; Motornov, M.; Minko, S. *Langmuir* **2008**, *24*, 13828–13832. (m) Lin, Y. H.; Teng, J.; Zubarev, E. R.; Shulha, H.; Tsukruk, V. V. *Nano Lett.* **2005**, *5*, 491–495.

(12) (a) Zhao, B. *Polymer* **2003**, *44*, 4079–4083. (b) Zhao, B. *Langmuir* **2004**, *20*, 11748–11755. (c) Zhao, B.; He, T. *Macromolecules* **2003**, *36*, 8599–8602. (d) Zhao, B.; Haasch, R. T.; MacLaren, S. *J. Am. Chem. Soc.* **2004**, *126*, 6124–6134. (e) Zhao, B.; Haasch, R. T.; MacLaren, S. *Polymer* **2004**, *45*, 7979–7988. (f) Li, D. J.; Sheng, X.; Zhao, B. *J. Am. Chem. Soc.* **2005**, *127*, 6248–6256. (g) Santer, S.; Kopyshev, A.; Donges, J.; Rühe, J.; Jiang, X. G.; Zhao, B.; Müller, M. *Langmuir* **2007**, *23*, 279–285.

(13) (a) Chiu, J. J.; Kim, B. J.; Kramer, E. J.; Pine, D. J. *J. Am. Chem. Soc.* **2005**, *127*, 5036–5037. (b) Shan, J.; Nuopponen, M.; Jiang, H.; Viitala, T.; Kauppinen, E.; Kontturi, K.; Tenhu, H. *Macromolecules* **2005**, *38*, 2918–2926. (c) Zubarev, E. R.; Xu, J.; Sayyad, A.; Gibson, J. D. *J. Am. Chem. Soc.* **2006**, *128*, 4958–4959. (d) Guo, Y.; Moffitt,

M. G. *Macromolecules* **2007**, *40*, 5868–5878. (e) Cheng, J.; He, J.; Li, C.; Yang, Y. *Chem. Mater.* **2008**, *20*, 4224–4230.
(14) Minko, S.; Luzinov, I.; Luchnikov, V.; Müller, M.; Patil, S.; Stamm, M. *Macromolecules* **2003**, *36*, 7268–7279.
(15) Hamley, I. W. *The Physics of Block Copolymers*; Oxford University Press: Oxford, 1998.
(16) Zhao, B.; Zhu, L. *J. Am. Chem. Soc.* **2006**, *128*, 4574–4575.
(17) Zhu, L.; Zhao, B. *J. Phys. Chem. B* **2008**, *112*, 11529–11536.
(18) Hawker, C. J.; Bosman, A. W.; Harth, E. *Chem. Rev.* **2001**, *101*, 3661–3688.
(19) (a) Motornov, M.; Sheparovych, R.; Lupitskyy, R.; MacWilliams, E.; Hoy, O.; Luzinov, I.; Minko, S. *Adv. Funct. Mater.* **2007**, *17*, 2307–2314. (b) Motornov, M.; Sheparovych, R.; Lupitskyy, R.; MacWilliams, E.; Minko, S. *J. Colloid Interface Sci.* **2007**, *310*, 481–488.
(20) Matyjaszewski, K.; Miller, P. J.; Shukla, N.; Immaraporn, B.; Gelman, A.; Luokala, B. B.; Siclovan, T. M.; Kickelbick, G.; Vallant, T.; Hoffmann, H.; Pakula, T. *Macromolecules* **1999**, *32*, 8716–8724.
(21) (a) Dao, J.; Benoit, D.; Hawker, C. J. *J. Polym. Sci., Part A: Polym. Chem.* **1998**, *36*, 2161–2167. (b) Zhao, B.; Jiang, X. M.; Li, D. J.; Jiang, X. G.; O'Lenick, T. G.; Li, B.; Li, C. Y. *J. Polym. Sci., Part A: Polym. Chem.* **2008**, *46*, 3438–3446.
(22) (a) Philipse, A. P.; Vrij, A. *J. Colloid Interface Sci.* **1989**, *128*, 121–136. (b) Bogush, G. H.; Tracy, M. A.; Zukoski, C. F., IV *J. Non-Cryst. Solids* **1988**, *104*, 95–106.
(23) Husseman, M.; Malmstrom, E. E.; McNamara, M.; Mate, M.; Mecerreyes, D.; Benoit, D. G.; Hedrick, J. L.; Mansky, P.; Huang, E.; Russell, T. P.; Hawker, C. J. *Macromolecules* **1999**, *32*, 1424–1431.
(24) (a) Tunca, U.; Karliga, B.; Ertekin, S.; Ugur, A. L.; Sirkecioglu, O.; Hizal, G. *Polymer* **2001**, *42*, 8489–8493. (b) Tunca, U.; Erdogan, T.; Hizal, G. *J. Polym. Sci., Part A: Polym. Chem.* **2002**, *40*, 2025–2032.
(25) Hiemenz, P. C.; Lodge, T. P. *Polymer Chemistry*, 2nd ed.; CRC Press: Boca Raton, FL, 2007.
(26) (a) Chen, W. Y.; Zheng, J. X.; Cheng, S. Z. D.; Li, C. Y.; Huang, P.; Zhu, L.; Xiong, H. M.; Ge, Q.; Guo, Y.; Quirk, R. P.; Lotz, B.; Deng, L. F.; Wu, C.; Thomas, E. L. *Phys. Rev. Lett.* **2004**, *93*, 028301. (b) Zheng, J. X.; Xiong, H. M.; Chen, W. Y.; Lee, K.; Van Horn, R. M.; Quirk, R. P.; Lotz, B.; Thomas, E. L.; Shi, A.-C.; Cheng, S. Z. D. *Macromolecules* **2006**, *39*, 641–650.
(27) Savin, D. A.; Pyun, J.; Patterson, G. D.; Kowalewski, T.; Matyjaszewski, K. *J. Polym. Sci., Part B: Polym. Phys.* **2002**, *40*, 2667–2676.
(28) The density of P*t*BA was not found in the literature. We used the density of poly(*tert*-butyl methacrylate) (1.03 g/cm^3) in the calculation. The density of PS is 1.05 g/cm^3.
(29) Bates, F. S. *Science* **1991**, *251*, 898–905.
(30) Feng, C. L.; Vancso, G. J.; Schonherr, H. *Langmuir* **2005**, *21*, 2356–2363.
(31) Mark, J. E. *Physical Properties of Polymers Handbook*; AIP Press: New York, 1996.